JOC The Journal of Organic Chemistry

Article

pubs.acs.org/joc

Reactions of C_{70}^{2-} with Organic Halides Revisited: Unusual Magnetic Equivalence for the Diastereotopic Methylene Protons in 2,5-$(PhCH_2)_2C_{70}$

Shu-Hui Li, Zong-Jun Li, Wei-Wei Yang, and Xiang Gao*

State Key Laboratory of Electroanalytical Chemistry, Changchun Institute of Applied Chemistry, University of Chinese Academy of Sciences, Chinese Academy of Sciences, 5625 Renmin Street, Changchun, Jilin 130022, China

Supporting Information

ABSTRACT: The reactions of C_{70}^{2-} with organic halides result in several isomeric products. However, the structures of the isomers have not been identified unambiguously and the reactions still remain elusive even though the first report of the reaction appeared more than ten years ago. Herein, the reactions of C_{70}^{2-} with $ArCH_2Br$ (Ar = Ph, *o*-, *m*-, and *p*-BrC_6H_4) are revisited. Two types of isomeric *para*-adducts of 2,5- and 7,23-$(ArCH_2)_2C_{70}$ are obtained and characterized with the X-ray single-crystal diffractions, HRMS, ^1H and ^{13}C NMR, and UV−vis spectroscopies. An unusual singlet resonance instead of the typical AB quartet resonance is shown for the C2 diastereotopic methylene protons in ^1H NMR spectrum of 2,5-$(PhCH_2)_2C_{70}$ recorded at ambient temperature. The unexpected magnetic equivalence is studied with the variable-temperature (VT) NMR and density functional theory (DFT) calculations. The results show that the greater local curvature in the C_{70} polar region is likely responsible for the unusual magnetic equivalence exhibited by the C2 diastereotopic methylene protons of 2,5-$(PhCH_2)_2C_{70}$, indicating that under certain cases, it is improbable to elucidate the spectral data of fullerene derivatives with a less symmetrical carbon cage in analogy with those of the C_{60} derivatives.

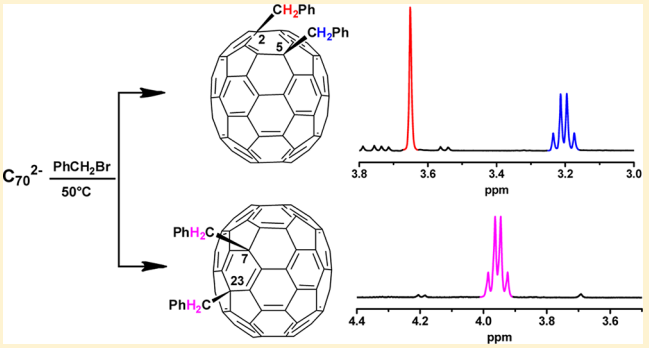

INTRODUCTION

The reactions of anionic fullerene species[1−24] are important supplements to the reactions of neutral fullerenes.[25] Neutral fullerenes are quite electron-deficient as evidenced by the electrochemical study, where C_{60} and C_{70} undergo six consecutive one-electron transfer reductions,[26] and they are typically involved in the reactions with nucleophiles.[25] As for the anionic fullerenes, they are electron-rich species and tend to undergo reactions with electrophiles.[1−24] Because of the electron-deficiency of fullerenes, anionic fullerenes are stable and readily available via either electrochemical[1−6,16−18,23,24] or chemical[7−15,19−22] reductions.

The most conventional reactions studied for the anionic fullerenes are the reactions of C_{60} dianion with organic halides,[1−4,7−15] which would form either the 1,4-adducts (*para*-configuration, addition occurs at the carbon atoms across one hexagon of fullerenes) or 1,2-adducts (*ortho*-configuration, addition takes place at the carbon atoms between two hexagons of fullerenes) depending on the size of addends, as a result of the intrinsic stability difference between the two types of adducts and the instability caused by the steric hindrance when the addends are closely positioned.[27] However, the reactions of C_{70}^{2-} with organic halides have remained elusive, even though the first report on the reaction of C_{70}^{2-} with $PhCH_2Br$ appeared more than 10 years ago,[16] because the structures of the products have not been identified unambiguously due to the structural complications caused by the lower symmetry of C_{70} cage.[28] For the reaction of C_{70}^{2-} with $PhCH_2Br$, three regioisomers were proposed to form on the basis of ^1H NMR results,[16] where two AB quartets and one singlet resonance are shown for the methylene protons of the benzyls. The two AB quartet resonances were assigned to the 7,23- (**1a**) and 7,19-adducts (Scheme 1), respectively, and the singlet resonance was assigned to the 7,38-adduct[29,30] (Scheme 1) by reasoning with the analogy of the ^1H NMR results of C_{60} derivatives and also computational calculations. However, only the 7,23-isomer has been identified explicitly by the ^{13}C INADEQUATE NMR using ^{13}C-enriched C_{70},[21] while the structures of the other products have never been confirmed.

Herein, we report the revisit of the reactions of C_{70}^{2-} with $ArCH_2Br$ (Ar = Ph, *o*-, *m*-, and *p*-BrC_6H_4). The reaction products have been structurally characterized with the X-ray single-crystal diffractions and various spectroscopic methods. The results show unambiguously that 7,23- (**1**) and 2,5-isomers (**2**) (Scheme 1) are obtained, while neither 7,19- nor 7,38-isomer is formed from the reaction. VT ^1H NMR and computational calculations have also been performed to

Received: May 30, 2013
Published: June 25, 2013

   dx.doi.org/10.1021/jo4011848 | J. Org. Chem. 2013, 78, 7208−7215

Scheme 1. Illustrated Structures of the 7,19-, 7,38-, and 7,23-$(PhCH_2)_2C_{70}$ Adducts Claimed in Ref 16 and the C_{70} 7,23-Adduct (1) and 2,5-Adduct (2) Obtained in This Work

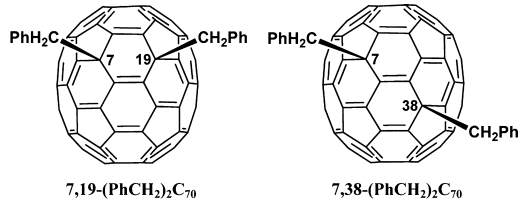

7,19-$(PhCH_2)_2C_{70}$ 7,38-$(PhCH_2)_2C_{70}$

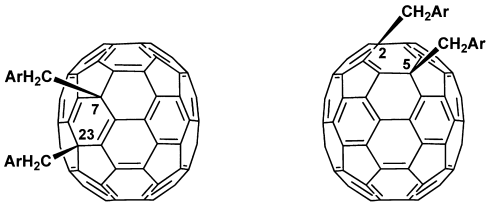

1 **2**

1a: Ar = Ph
1b: Ar = *o*–BrC_6H_4
1c: Ar = *m*–BrC_6H_4
1d: Ar = *p*–BrC_6H_4

2a: Ar = Ph
2b: Ar = *o*–BrC_6H_4
2c: Ar = *m*–BrC_6H_4
2d: Ar = *p*–BrC_6H_4

rationalize the unusual magnetic equivalence shown in the ^1H NMR spectrum of 2,5-$(PhCH_2)_2C_{70}$, which has confused the previous assignment of the product.

RESULTS AND DISCUSSION

Reactions of C_{70}^{2-} with $ArCH_2Br$ (Ar = Ph, *o*-, *m*-, *p*-BrC_6H_4) and Structural Characterizations of the Products. The reactions of C_{70}^{2-} with organic halides were carried out following procedures reported previously,[16] except the reaction temperature was elevated to 50 °C to improve the yield of the products (see the Experimental Section). The crude mixture consists of two major products, which are identified as the 7,23-$(ArCH_2)_2C_{70}$ (**1**) and 2,5-$(ArCH_2)_2C_{70}$ (**2**) after a two-stage HPLC purification, along with unreacted C_{70}.

Single-crystals suitable for X-ray diffractions have been obtained for **1b**, **1c**, **2a**, and **2d**. Figure 1 displays the ORTEP diagrams of the resolved structures of **1b**, **1c**, **2a**, and **2d**, which unambiguously show that two types of *para*-adducts, 7,23- and 2,5-isomers, are produced from the reactions of C_{70}^{2-} with organic halides, consistent with the addition preference of benzyls when reacting with fullerene cages of C_{60}[3,4] and $M_3N@C_{80}$ (M = Lu, Sc).[31] Notably, the phenyl rings in each compound are all located over a hexagon of C_{70}, suggesting a possible interaction between the phenyl ring and the hexagon of C_{70} cage. To the best of our knowledge, this is the first time that single-crystal structures for the C_{70} 7,23- and 2,5-adducts have been obtained, and they may provide more structural details for the 7,23-isomer and also the 2,5-isomer, which has been proposed for C_{70} derivatives with addends of *tert*-butylperoxo[32] and trifluoromethyl[33] on the basis of molecule symmetry and computational calculations.

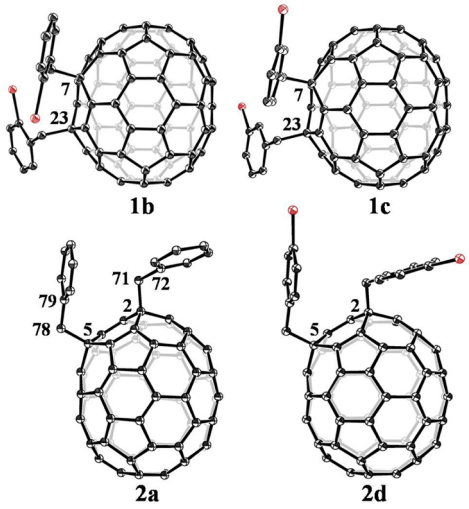

Figure 1. ORTEP diagrams for **1b**, **1c**, **2a**, and **2d** molecules with 30% thermal ellipsoids. The solvent molecules and hydrogen atoms are omitted for clarity.

The HRMS of **1a**–**d** and **2a**–**d** (see the Supporting Information) show M^+ or $[M + H]^+$ at 1022.11086, 1177.93290, 1178.93294, 1178.93607 and 1023.11635, 1178.93590, 1178.94001, 1178.93639, respectively, consistent with the formation of the respective $(ArCH_2)_2C_{70}$ molecules. Compounds **1a** and **1d** are identified as the 7,23-adducts, while compounds **2b** and **2c** are determined as the 2,5-adducts by comparing the UV–vis absorptions with **1b**,**c** and **2a**,**d**, respectively, since UV–vis spectroscopy has been shown to be characteristic of the addition pattern rather than the types of addends.[34] The ^{13}C NMR spectra of **1a**–**d** (see the Supporting Information) all display a similar pattern, with one resonance for the methylene carbon (around 50 ppm) of the benzyl and one resonance for the sp^3 C_{70} carbon (around 56 ppm) bonded to the benzyl for each compound, and a total of about 32 sp^2 C_{70} resonances along with signals arising from the phenyl rings, consistent with the C_2 symmetry of the 7,23-adduct. As for **2a**–**d**, the ^{13}C NMR spectra display two resonances for the methylene carbons, two signals for the sp^3 C_{70} carbons bonded to the benzyls for each compound, and a total of about 60 sp^2 C_{70} resonances along with signals due to the phenyl carbons, consistent with the C_1 symmetry of the 2,5-adduct as shown by the crystal structure.

^1H NMR of 2,5-$(PhCH_2)_2C_{70}$: Singlet Resonance for the C2 Diastereotopic Methylene Protons. The ^1H NMR spectra of the 7,23-adducts (**1a**–**d**) show one AB quartet for the two sets of diastereotopic methylene protons of each compound (see the Supporting Information), consistent the C_2 symmetry of the molecule and in agreement with the conventions exhibited by the diastereotopic methylene protons bonded to the C_{60}[3,12−15,35] and C_{80}[31] cages.

Surprisingly, a totally different scenario is shown for the ^1H NMR spectrum of 2,5-$(PhCH_2)_2C_{70}$ (**2a**). Figure 2a displays the expanded ^1H NMR spectrum (600 MHz) for the methylene protons of **2a** recorded at room temperature, which shows one AB quartet (δ = 3.20 ppm, AB_q, $\Delta\nu_{AB}$ = 24.0 Hz, J_{AB} = 18.0 Hz, 2H) and one singlet (δ = 3.65 ppm, 2H) resonances for the two sets of methylene protons, consistent with the result reported previously.[16] The presence of an AB quartet is quite typical for the diastereotopic methylene protons, as compared with the counterpart of **1a**–**1d** and also the adducts of C_{60}[3,12−15,35] and $M_3N@C_{80}$.[31] However, the appearance of a singlet resonance for the diastereotopic methylene protons at room temperature is really unexpected, especially by analyzing the ^1H NMR results of the diastereotopic methylene protons bonded to C_{60} and C_{80} cages and also to the C_{70} cage at the equatorial 7,23-positions. Previous work has shown that the diastereotopic methylene protons of 1,4-$(PhCH_2)_2C_{60}$ would exhibit a broad

dx.doi.org/10.1021/jo4011848 | J. Org. Chem. 2013, 78, 7208–7215

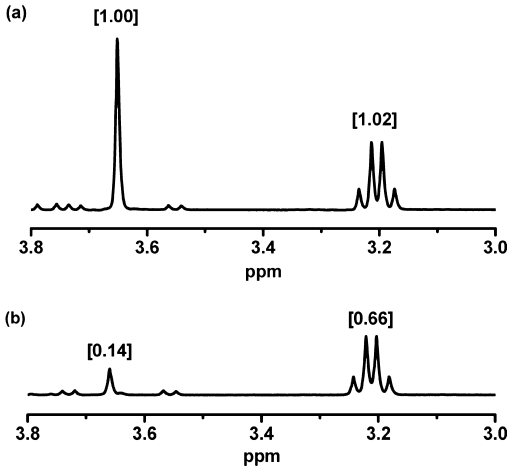

Figure 2. Expanded ^{1}H NMR spectra (600 Hz) of (a) **2a** and (b) **2f** showing the resonances of methylene protons recorded in CS_2 with benzene-d_6 as the external lock solvent at room temperature. The labeled numbers in brackets refer to the relative integration areas.

singlet resonance only at a high temperature of 370 K due to the coalesce of the AB quartet,[36] which is likely caused by the accelerated rotation of the phenyl rings, whose conformation significantly affects the magnetic equivalence of the diastereotopic methylene protons as shown in previous work.[37] This ambient singlet resonance was unfortunately misassigned to the 7,38-C_{70} adduct (Scheme 1), by assuming that the two far-separated benzyls might have much less interactions with each other and thus rotate in a rather free manner.[16,38]

Two H/D labeling experiments were carried out to identify which set of the diastereotopic methylene protons would exhibit the magnetic equivalence. The first one was performed by adding equal amounts of $PhCD_2Br$ and $PhCH_2Br$ ($n_{PhCD2Br}$:$n_{PhCH2Br}$:n_{C70} = 10:10:1) simultaneously into the C_{70}^{2-} solution, and the obtained 2,5-adduct is designated as **2e**. The second experiment was carried out by also using equal amounts of $PhCD_2Br$ and $PhCH_2Br$ ($n_{PhCD2Br}$:$n_{PhCH2Br}$:n_{C70} = 10:10:1), but with a stepwise addition manner, where $PhCD_2Br$ was added first, followed by the addition of $PhCH_2Br$ with a time interval of about 20 min (see the Experimental Section), similar to the procedures reported previously,[6,18,35] which can effectively differentiate the benzyls added during different steps of the reaction, by taking advantage of the stepwise nature of the reaction between the dianion of fullerenes and organic halides.[8,10,16,17] The obtained 2,5-adduct is designated as **2f**.

No significant SKIE (secondary kinetic isotope effect) is observed between $PhCH_2Br$ and $PhCD_2Br$ as indicated by the ^{1}H NMR spectrum of **2e** (Figure S39, Supporting Information), which shows both the singlet and the AB quartet resonances consist of almost equal amount of $PhCD_2$ and $PhCH_2$. As for compound **2f**, the ^{1}H NMR spectrum (Figure 2b) shows that the singlet resonance has a much lower intensity with respect to the AB quartet, indicating explicitly that the singlet originates from the benzyl added to C_{70}^{2-} during the first step. Previous work has demonstrated that C2 is the first addition site since the C2-RC_{70}^- is more stable;[17,18,39] the results therefore show unambiguously that the C2 diastereotopic methylene protons are the ones exhibiting the singlet resonance in the ^{1}H NMR spectrum, while the C5 diastereotopic methylene protons still exhibit the typical AB quartet signal.

Compounds 2,5-$(ArCH_2)_2C_{70}$ (Ar = *o*-, *m*-, *p*-BrC_6H_4) (**2b**, **2c**, and **2d**) were also subjected to the ^{1}H NMR characterization (see the Supporting Information). Different from the result of 2,5-$(PhCH_2)_2C_{70}$, the two sets of the methylene protons both display AB quartets for the C_{70} derivatives with the Br-substituted benzyls, implying that the exhibited magnetic equivalence for the C2 diastereotopic methylene protons of 2,5-$(PhCH_2)_2C_{70}$ is rather delicate.

VT ^{1}H NMR and DFT Computational Calculations. To obtain a better understanding on the exhibited magnetic equivalence of the C2 diastereotopic methylene protons of **2a**, VT ^{1}H NMR was performed on the 2,5-$(PhCH_2)_2C_{70}$, and the results are displayed in Figure 3. As is shown in the Figure,

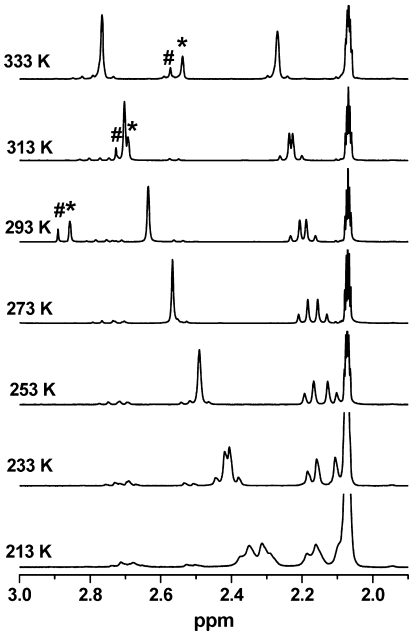

Figure 3. Expanded VT ^{1}H NMR spectra (600 Hz) of 2,5-$(PhCH_2)_2C_{70}$ from 213 to 333 K recorded in CS_2 with acetone-d_6 as the external lock solvent. The signals labeled with # and * in the spectra (from 293 to 333 K) are likely due to the H_2O residue presented in CS_2 and acetone-d_6.

when the temperature is low (213 and 233 K), the C2 diastereotopic methylene protons indeed exhibit an AB quartet; while as the temperature reaches to 253 K and above, the C2 methylene protons exhibit a singlet resonance despite of their diastereotopic nature. The results indicate that the exhibited magnetic equivalence for the C2 diastereotopic methylene protons at room temperature is likely caused by the same mechanism that coalesces the AB quartet of 1,4-$(PhCH_2)_2C_{60}$ at high temperature, i.e., the rapid rotation of the phenyl ring,[37] suggesting that the barrier for the rotation of phenyl ring of the C2 benzyl about the C71−C72 bond (Figure 1 for **2a**) is less than that for rotating the phenyl ring of the C5 benzyl about the C78−C79 bond (Figure 1 for **2a**) and also the one for rotating the phenyl ring in 1,4-$(PhCH_2)_2C_{60}$. Notably, the AB quartet signal due to the C5 methylene protons also coalesces into a singlet resonance as the temperature is increased to 333 K, suggesting that the barrier for the rotation of the phenyl ring of the C5 benzyl about the C78−C79 bond is also less than the respective one for rotating the phenyl ring in 1,4-$(PhCH_2)_2C_{60}$.

DFT calculations were performed to rationalize the much less rotational barrier for the C2 phenyl around the C2−C71

dx.doi.org/10.1021/jo4011848 | J. Org. Chem. 2013, 78, 7208−7215

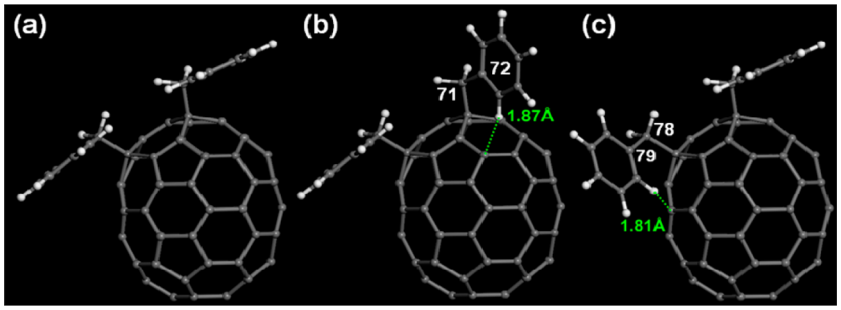

Figure 4. (a) Simulated structure of 2,5-$(PhCH_2)_2C_{70}$ used for calculations of the rotational barriers of the phenyl rings about the C71−C72 and C78−C79 bonds; (b) the most hindered structures simulated by the rotation of the C2 phenyl; (c) the most hindered structures simulated by the rotation of the C5 phenyl.

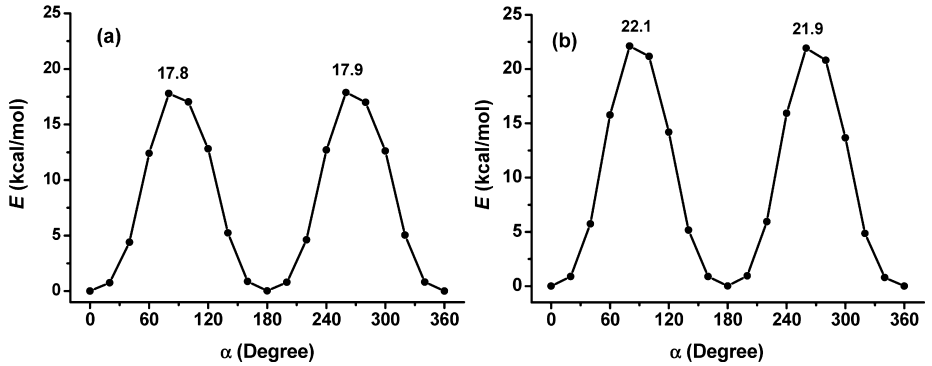

Figure 5. Calculated energy profiles on the rotation of the phenyl ring of (a) the C2 phenyl about the C71−C72 bond and (b) the C5 phenyl about the C78−C79 bond.

bond. The geometry of the simulated structures were optimized at the HF/6-31G level, and the rotational barriers were calculated at the B3LYP/6-311G(d) level. It is noteworthy that if a structure with the conformation similar to the crystal structure of **2a** (Figure 1), where the C5 benzyl is orientated toward the C2 benzyl, is directly used for the simulation, the C5 phenyl ring would experience a significant hindrance from the interactions with the methylene protons of the C2 benzyl during the simulated rotation due to the specific conformation of the benzyls, indicating that it is unlikely for the C5 phenyl ring to rotate over the hexagon located in the polar region, rather the C5 phenyl ring would be likely to rotate over the hexagon in the equatorial region, if such a configuration is also an energy minimum and the rotation barrier for the C5 benzyl about the C5−C78 bond (Figure 1, **2a**) is small enough.

The evaluation of the rotation hindrance of respective benzyl about the C2−C71 and C5−C78 bonds is therefore necessary before assessing the rotational barriers of the C2 and C5 phenyl rings about the C71−C72 and C78−C79 bonds. Simulated molecules of 2,5-$(PhCH_2)HC_{70}$ and 2,5-$H(PhCH_2)C_{70}$ were used to avoid the overestimation of the hindrance brought by the interactions between the two benzyls if 2,5-$(PhCH_2)_2C_{70}$ was used. The simulated molecules of 2,5-$(PhCH_2)HC_{70}$ and 2,5-$H(PhCH_2)C_{70}$ were constructed on the basis of the optimized structure starting with the crystal structure of **2a**, where one benzyl was replaced with an H atom, while the other benzyl was remained with the original conformation. A small hindrance of 4.9 and 6.8 kcal/mol is predicted for the rotation of the C2 and C5 benzyls about the C2−C71 and C5−C78 bond, respectively (see Figures S48 and S49, Supporting Information, for the calculated energy profiles), suggesting that it is possible for the C2 and C5 benzyl to adopt conformation other than the one shown in the single-crystal structure.

The rotational barrier calculations for the C2 and C5 phenyl about the C71−C72 bond and C78−C79 bonds were performed by adopting a configuration as shown in Figure 4a, where the C2 benzyl remains the similar conformation as that shown in the crystal structure of **2a**, while the C5 benzyl is rotated over the equatorial hexagon of C_{70} that contains C5 for the following reasons: First, the rotation barrier of the C5 benzyl about the C5−C78 bond is quite small, and such a configuration is also an energy minimum, with only about 0.4 kcal/mol higher than the optimized configuration starting with the single-crystal structure; second, with such conformation, it would avoid the interactions between the two benzyls during the simulated rotation of the C5 phenyl, suggesting that this is more likely the actual rotation pathway for the C5 phenyl about the C78−C79 bond.

Parts b and c of Figure 4 show the diagrams of the most hindered structures simulated by the rotation of the phenyl rings of the C2 and C5 benzyls, respectively. As is shown in Figure 4, the rotation hindrance mainly arises from the interactions of the phenyl ring with the C_{70} fullerene cage. The shortest distance between the *ortho* H of C2 phenyl and C_{70} cage is 1.87 Å, while it is 1.81 Å between the *ortho* H of C5 phenyl and the C_{70} cage, suggesting a smaller barrier for the rotation of the C2 phenyl than rotating the C5 phenyl.

Figure 5 shows the calculated energy profiles for the rotation of the C2 and C5 phenyls about the C71−C72 and C78−C79 bonds. The calculations predict a barrier of about 17.8 kcal/mol for the rotation of the C2 phenyl, and 21.9 kcal/mol for the rotation of the C5 phenyl, consistent with the experimental results that the C2 diastereotopic methylene protons exhibit a

dx.doi.org/10.1021/jo4011848 | J. Org. Chem. 2013, 78, 7208−7215

Scheme 2. Proposed Mechanism for the Reaction of C_{70}^{2-} with Organic Halides

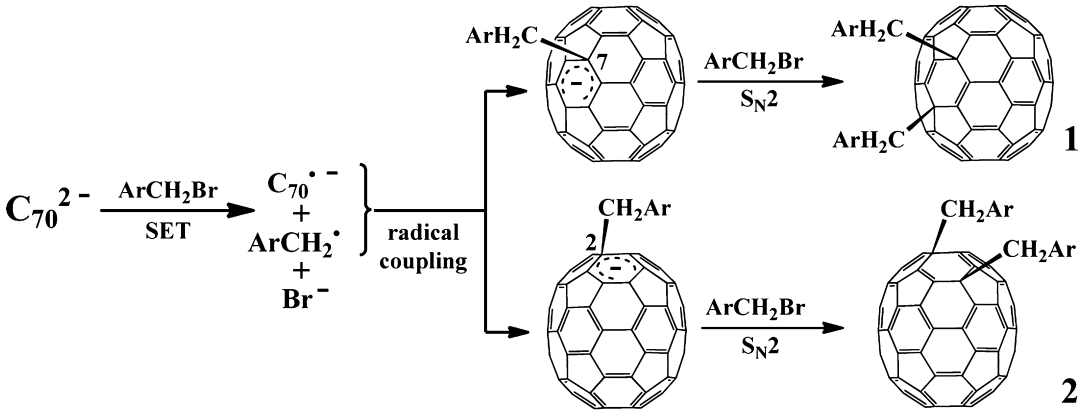

singlet resonance, while the C5 ones exhibit an AB quartet resonance in the ^{1}H NMR spectrum for the compound and also the simulated most hindered structures shown in parts b and c of Figure 4.

The results indicate that the unusual magnetic equivalence observed for the C2 methylene protons of 2,5-$(PhCH_2)_2C_{70}$ is likely caused by the free rotation of the C2 phenyl ring due to a small rotation hindrance. Such a small barrier is probably related to the specific shape of C_{70} carbon cage, where the polar region has the greatest curvature, while the equatorial region is much flatted. As is shown in parts b and c of Figure 4, the C2 phenyl is likely to have an interaction with the hexagon located in the polar region, while the C5 phenyl would be likely have an interaction with the hexagon in the equatorial region during their respective rotation. Consequently, the C2 phenyl would have a longer distance from the carbon cage due to the greater curvature of the fullerene cage and experiences a less rotation hindrance, while the C5 phenyl would be likely to have a shorter distance from the carbon cage due to the flat surface of equatorial region of C_{70}, and experiences a greater rotation hindrance. Notably, no such structural variance is encountered for the spherical cages such as C_{60} and C_{80} with I_h symmetry, suggesting that an addend bonded to a spherical carbon cage may experience a different effect compared with the addend bonded to a less symmetrical carbon cage, indicating that cautions should be taken when structural elucidations of fullerene derivatives with a less symmetrical carbon cage by reasoning in analogy with the spectral results of C_{60} derivatives.

As for the Br-substituted 2,5-adducts, the Br may slightly change the conformations of the aromatic rings, thus varying the barrier for the rotation of the C2 phenyl, and results in the exhibition of AB quartet resonance for the respective C2 methylene protons.

Reaction Mechanism of C_{70}^{2-} with Organic Halides. On the basis of the product structures and previous work on the reaction of fullerene dianions,[8,10,16,17] the reactions of C_{70}^{2-} with organic halides are finally clarified, and a reaction mechanism for the formation of diorgano C_{70} *para*-adducts is proposed as shown in Scheme 2. A single-electron transfer (SET) occurs between C_{70}^{2-} and $ArCH_2Br$ with the formation of $C_{70}^{\bullet-}$ and $ArCH_2^{\bullet}$, which consequently form the C2−RC_{70}^- and C7−RC_{70}^- intermediates via radical coupling reaction owing to the stability of these two species as supported by the DFT calculations.[17] A subsequent *para*-addition of the second benzyl would then take place via the S_N2 attack of C2−RC_{70}^- or C7−RC_{70}^- to $ArCH_2Br$, resulting in the 2,5- and 7,23-isomers.

CONCLUSION

The reactions of C_{70}^{2-} with organic halides have been reinvestigated, and the reaction products have been identified with the X-ray single-crystal diffractions and various spectroscopic characterizations. Experiment of H/D labeling has identified the C2 diastereotopic methylene protons of 2,5-$(PhCH_2)_2C_{70}$ as the ones that exhibit the singlet resonance, and such unusual magnetic equivalence is further studied with the VT ^{1}H NMR and DFT calculations. The results imply that the curvature variance of a fullerene carbon cage may affect the ^{1}H NMR spectra of the derivatives, indicating that cautions should be exercised when structural elucidations of fullerene derivatives with a less symmetrical carbon cage by reasoning in analogy with the ^{1}H NMR results of C_{60} derivatives. The understanding of the effect of less symmetrical fullerene carbon cages toward the ^{1}H NMR of the fullerene derivatives is of significance, since the carbon cages of most higher fullerenes are less symmetrical, and the study of the chemical reactivity of higher fullerenes has been considered as one of the new challenges in the fullerene chemistry,[40] where the ^{1}H NMR spectroscopy is expected to play an important role, because it requires much less samples than the ^{13}C NMR and the availability of higher fullerenes is very limited at current stage.

EXPERIMENTAL SECTION

General Methods. All reactions were carried out under an atmosphere of argon. All reagents were obtained commercially and used without further purification unless otherwise noted. Benzonitrile (PhCN) was distilled over P_2O_5 under vacuum at 305 K prior to use. Tetra-*n*-butylammonium perchlorate (TBAP) was recrystallized from absolute ethanol and dried under vacuum at 313 K prior to use.

Controlled-potential bulk electrolysis was carried out on a potentiostat/galvanostat using an "H" type cell which consisted of two platinum gauze electrodes (working and counter electrodes) separated by a sintered glass frit. A saturated calomel electrode (SCE) was used as reference electrode. A fritted-glass bridge of low porosity which contained the solvent/supporting electrolyte mixture was used to separate the SCE from the bulk of the solution.

Synthesis of 7,23- and 2,5-$(ArCH_2)_2C_{70}$ (Ar = Ph, *o*-, *m*-, and *p*-BrC_6H_4). Typically, C_{70} (100 mg, 0.12 mmol) was electrolyzed at −1.10 V versus SCE in freshly distilled PhCN solution containing 0.1 M TBAP under an argon atmosphere. The potentiostat was switched off after the electrolytic formation of C_{70}^{2-} was complete, and a 50-fold excess of $ArCH_2Br$ was added into the solution under inert atmosphere. The reaction was allowed to proceed for about 3 h

dx.doi.org/10.1021/jo4011848 | J. Org. Chem. 2013, 78, 7208−7215

with stirring at 50 °C. The mixture was dried with a rotary evaporator under reduced pressure, and the residue was washed with methanol to remove TBAP and excessive $ArCH_2Br$. The obtained crude mixture was put into toluene and sonicated for 10 min, and the soluble part was further purified by HPLC over a two-stage chromatographic procedure. At the first stage, the crude mixture was eluted with toluene over a semipreparative Buckyprep column with a flow rate of 3.7 mL/min, and the two fractions of the products were collected together. At the second stage, the collected product mixture during the first stage was eluted with a mixture of toluene and *n*-hexane (v:v = 7:3) over a semipreparative Buckyprep column. Satisfactory separations of **1a** from **2a** and **1b** from **2b** were achieved when the flow rate was 3.7 mL/min; and satisfactory separations of **1c** from **2c** and **1d** from **2d** were achieved when the flow rate was 2.5 mL/min. Under typical conditions, the isolated yield for the 7,23-$(ArCH_2)_2C_{70}$ is 33% (40 mg) for **1a**, 21% (29 mg) for **1b**, 24% (34 mg) for **1c**, and 33% (46 mg) for **1d**; while it is 36% (44 mg) for **2a**, 31% (43 mg) for **2b**, 35% (49 mg) for **2c**, and 26% (36 mg) for **2d**. The recovery yield of C_{70} is 18% (18 mg), 26% (26 mg), 27% (27 mg), and 26% (26 mg) for the reactions of C_{70}^{2-} with $PhCH_2Br$ and *o*-, *m*-, *p*-$BrC_6H_4CH_2Br$ respectively. No data on the melting point of the C_{70} derivatives could be obtained, since the compounds would decompose before reaching to the melting point.

Spectral Characterization of 1a. Positive ESI FT-ICR MS: *m*/*z* calcd for M^+ ($C_{84}H_{14}^+$) 1022.10900, found 1022.11086. ^{1}H NMR (600 MHz, in CS_2 with benzene-d_6 as the external lock solvent) δ = 7.62−7.56 (m, 10H), 3.96 (AB_q, $\Delta\nu$ = 24.0 Hz, J = 18.0 Hz, 4H). ^{13}C NMR (125 MHz, CS_2/$CDCl_3$): δ = 158.35 (2C), 151.12 (2C), 150.66 (2C), 150.58 (2C), 149.82 (2C), 148.93 (2C), 148.85 (2C), 148.72 (2C), 148.50(2C), 148.39 (2C), 147.49 (2C), 147.38 (2C), 147.16 (2C), 147.09 (2C), 146.97 (2C), 146.21 (2C), 146.00 (2C), 145.45 (2C), 145.35 (2C), 145.29 (2C), 144.92 (2C), 144.63 (2C), 144.42 (2C), 143.74 (2C), 143.20 (2C), 142.96 (2C), 142.18 (2C), 141.25 (2C), 140.14 (2C), 139.44 (2C), 135.71 (2C,Ph), 134.24 (2C), 134.17 (2C), 133.71 (2C), 132.19 (2C), 130.68 (4C, Ph), 128.48 (4C, Ph), 127.71 (2C, Ph), 57.48 (2C, sp^3), 50.04 (2C, CH_2). UV−vis (toluene): λ_{max}/nm = 403, 438, 624, and 785.

Spectral Characterization of 2a. Positive ESI FT-ICR MS: *m*/*z* calcd for $[M + H]^+$ ($C_{84}H_{15}^+$) 1023.11683, found 1023.11635. ^{1}H NMR (600 MHz, in CS_2 with C_6D_6 as the external lock solvent) δ = 7.72 (d, 2H), 7.68 (t, 2H), 7.56 (t, 1H), 7.52 (t, 2H), 7.44 (t, 1H), 7.38 (d, 2H), 3.65 (s, 2H), 3.20 (AB_q, $\Delta\nu$ = 24.0 Hz, J = 18.0 Hz, 2H). ^{13}C NMR (150 MHz, in CS_2 with DMSO- d_6 as the external lock solvent) all signals represent 1C except noted: δ = 168.52, 159.59, 156.25, 154.22, 151.16, 150.97, 150.40, 149.79, 149.61, 149.19, 149.05, 149.02, 148.48 (2C), 148.37 (2C), 147.80 (2C), 147.40, 147.19, 147.14, 147.01 (2C), 146.93, 146.83, 146.76, 146.35, 146.12,146.97, 145.95, 145.68, 145.51, 145.38, 145.01 (2C), 144.81, 144.52 (2C), 144.26, 144.19, 143.87, 143.82, 143.67, 143.48, 143.16, 143.03, 142.97, 142.37, 142.20, 142.04, 142.02, 141.85, 141.52, 140.95, 138.29, 136.81, 136.41, 136.06 (2C), 135.70 (2C), 135.31, 133.83, 132.22, 132.18, 132.00, 131.62, 130.55, 130.25 (2C, Ph), 129.91 (2C, Ph), 129.02 (Ph), 128.31 (Ph), 127.87 (2C, Ph), 127.62 (2C, Ph), 126.82 (Ph), 126.77 (Ph), 57.23 (sp^3, C_{70}), 55.67 (sp^3, C_{70}), 46.31 (CH_2), 42.85 (CH_2). UV−vis (toluene): λ_{max}/nm =355, 415, 602, and 701.

X-ray Single-Crystal Diffraction of 2a. Black crystals of **2a** were obtained by slowly diffusing ethanol into a CS_2 solution of **2a** at room temperature. Single-crystal X-ray diffraction data were collected on an instrument equipped with a CCD area detector using graphite-monochromated Mo Kα radiation (λ = 0.71073 Å) in the scan range 1.19° < θ < 25.05°. The structure was solved with the direct method of SHELXS-97 and refined with full-matrix least-squares techniques using the SHELXL-97 program within WINGX. Crystal data of **2a**·CS_2: $C_{84}H_{14}$·CS_2, M_w = 1099.10, monoclinic, space group $P2(1)/c$, a = 19.190(3) Å, b = 13.797(2) Å, c = 19.557(2) Å, α = 90°, β = 120.635(11)°, γ = 90°, V = 4455.3(11) Å^3, Z = 4, D_{calcd} = 1.639 Mg m^{-3}, μ = 0.184 mm^{-1}, T = 188(2) K, crystal size 0.28 × 0.18 × 0.14 mm; reflections collected 24446, independent reflections 7864; 3297 with $I > 2\sigma(I)$; $R1$ = 0.1412 [$I > 2\sigma(I)$], w$R2$ = 0.2409 [$I > 2\sigma(I)$]; $R1$ = 0.2668 (all data), w$R2$ = 0.2877 (all data), GOF (on F^2) = 0.992.

Spectral Characterization of 1b. Positive ESI FT-ICR MS: *m*/*z* calcd for M^+ ($C_{84}H_{12}Br_2^+$), 1177.93003; found, 1177.93290. ^{1}H NMR (600 MHz, in CS_2 with benzene-d_6 as the external lock solvent) δ = 7.86 (d, 2H), 7.66 (d, 2H), 7.57 (t, 2H), 7.47 (t, 2H), 4.18 (AB_q, $\Delta\nu$ = 48.0 Hz, J = 12.0 Hz, 4H). ^{13}C NMR (125 MHz, CS_2/$CDCl_3$): δ = 157.83 (2C), 151.76 (2C), 150.83 (2C), 150.43 (2C), 149.75 (2C), 149.00 (2C), 148.84 (2C), 148.72 (2C), 148.54 (2C), 148.38 (2C), 147.53 (2C), 147.36 (2C), 147.21 (2C), 147.07 (2C), 146.94 (2C), 146.20 (2C), 146.04 (2C), 145.35 (2C), 145.32 (2C), 145.28 (2C), 144.64 (2C), 144.54 (2C), 144.40 (2C), 144.00 (2C), 142.89 (2C), 142.43 (2C), 142.16 (2C), 141.19 (2C), 139.54 (2C), 139.35 (2C), 135.59 (2C, Ph), 134.21 (2C), 134.18 (2C), 133.70 (2C), 133.66 (2C, Ph), 132.80 (2C, Ph), 132.28 (2C), 129.25 (2C, Ph), 127.19 (2C, Ph), 126.33 (2C, Ph) 56.95 (2C, sp^3, C_{70}), 47.84 (2C, CH_2). UV−vis (toluene): λ_{max}/nm = 403, 438, 624, and 785.

X-ray Single-Crystal Diffraction of 1b. Black crystals of **1b** were obtained by slowly diffusing ethanol into a CS_2 solution of **1b** at room temperature. Single-crystal X-ray diffraction data were collected on an instrument equipped with a CCD area detector using graphite-monochromated Mo Kα radiation (λ = 0.71073 Å) in the scan range 1.35° < θ < 26.11°. The structure was solved with the direct method of SHELXS-97 and refined with full-matrix least-squares techniques using the SHELXL-97 program within WINGX. Crystal data of **1b**·CS_2: $C_{84}H_{12}Br_2$·CS_2, M_w = 1256.89, monoclinic, space group $P2(1)/c$, a = 14.0028(8) Å, b = 10.9052(5) Å, c = 30.6099(16) Å, α = 90°, β = 98.8290(10)°, γ = 90°, V = 4618.6(4) Å^3, Z = 4, D_{calcd} = 1.808 Mg m^{-3}, μ = 1.910 mm^{-1}, T = 295(2) K, crystal size 0.39 × 0.26 × 0.21 mm; reflections collected 25222, independent reflections 9164; 5228 with $I > 2\sigma(I)$; $R1$ = 0.0857 [$I > 2\sigma(I)$], w$R2$ = 0.2337 [$I > 2\sigma(I)$]; $R1$ = 0.1481 (all data), w$R2$ = 0.2714 (all data), GOF (on F^2) = 1.104.

Spectral Characterization of 2b. Positive ESI FT-ICR MS: *m*/*z* calcd for $[M + H]^+$ ($C_{84}H_{13}Br_2^+$) 1178.93785, found 1178.93590. ^{1}H NMR (600 MHz, in CS_2 with benzene-d_6 as the external lock solvent) δ = 7.96 (d, 1H), 7.82 (d, 1H), 7.74 (d, 1H), 7.70 (t, 1H), 7.56−7.53(m, 2H), 7.49 (t, 1H), 7.36 (t, 1H), 4.00 (AB_q, $\Delta\nu$ = 144.0 Hz, J_{AB} = 12.0 Hz, 2H), 3.47 (AB_q, $\Delta\nu$ = 96.0) Hz, J_{AB} = 12.0 Hz, 2H). ^{13}C NMR (150 MHz, CS_2/$CDCl_3$) all signals represent 1C except noted: δ = 168.10, 159.45, 156.70, 154.71, 151.71, 151.51, 151.06, 150.38, 150.07, 149.59 (2C), 149.54, 149.05, 149.00, 148.85, 148.69, 148.36 (2C), 148.01, 147.72, 147.62, 147.57, 147.53, 147.44, 147.36, 147.29, 146.92, 146.75, 146.52, 146.48, 146.24, 146.06, 145.88, 145.53, 145.47, 145.33, 145.09, 144.94, 144.84, 144.72, 144.37, 144.36, 144.19, 143.76, 143.69, 143.55, 143.50, 142.89, 142.72, 142.60 (2C), 142.39, 142.04, 141.33, 138.80, 137.55, 136.87, 136.40, 135.86 (2C), 134.47, 133.44 (Ph), 133.13 (Ph), 132.77 (2C), 132.70 (Ph), 132.53, 132.45 (Ph), 132.16, 131.08, 130.76, 129.43, 129.06 (Ph), 128.94 (Ph), 128.74 (Ph), 128.15 (Ph), 127.29 (Ph), 127.02 (Ph), 126.33 (Ph), 125.97 (Ph), 56.96 (sp^3, C_{70}), 55.36 (sp^3, C_{70}), 45.65 (CH_2), 42.32 (CH_2). UV−vis (toluene): λ_{max}/nm =355, 415, 602, and 701.

Spectral Characterization of 1c. Positive ESI FT-ICR MS: *m*/*z* calcd for $[M + H]^+$ ($C_{84}H_{13}Br_2^+$) 1178.93785, found 1178.93924. ^{1}H NMR (600 MHz, in CS_2 with benzene-d_6 as the external lock solvent) δ = 7.69−7.66 (m, 4H), 7.51−7.47 (m, 4H), 3.86 (AB_q, $\Delta\nu$ = 24.0 Hz, J = 12.0 Hz, 4H). ^{13}C NMR (125 MHz, CS_2/$CDCl_3$): δ = 157.63 (2C), 150.95 (2C), 150.76 (2C), 150.50 (2C), 149.95 (2C), 148.94 (2C), 148.88 (2C), 148.84 (2C), 148.50 (2C), 148.47 (2C), 147.48 (2C), 147.36 (2C), 147.18 (4C), 147.01 (2C), 146.22 (2C), 146.07 (2C), 145.43 (2C), 145.37 (2C), 145.35 (2C), 144.74 (2C), 144.65 (2C), 144.52 (2C), 143.93 (2C), 143.05 (2C), 142.69 (2C), 142.35 (2C), 141.23 (2C), 139.81 (2C), 139.19 (2C), 137.89 (2C,Ph), 134.22 (2C), 134.19 (2C), 133.72 (2C), 133.57 (2C, Ph), 132.09 (2C), 130.91 (2C, Ph), 129.91 (2C, Ph), 129.12 (2C, Ph), 123.03 (2C, Ph), 56.99 (2C, sp^3, C_{70}), 49.44 (2C, CH_2). UV−vis (toluene): λ_{max}/nm = 403, 438, 624, and 785.

X-ray Single-Crystal Diffraction of 1c. Black crystals of **1c** were obtained by slowly diffusing *n*-hexane into a CS_2 solution of **1c** at room temperature. Single-crystal X-ray diffraction data were collected on an instrument equipped with a CCD area detector using graphite-monochromated Mo Kα radiation (λ = 0.71073 Å) in the scan range 1.90° < θ < 26.13°. The structure was solved with the direct method of

dx.doi.org/10.1021/jo4011848 | J. Org. Chem. 2013, 78, 7208−7215

SHELXS-97 and refined with full-matrix least-squares techniques using the SHELXL-97 program within WINGX. Crystal data of **1c**·0.5CS_2: $C_{84}H_{12}Br_2$·0.5CS_2, M_w = 1218.80, triclinic, space group *P*-1, *a* = 10.7742(8) Å, *b* = 11.1529(9) Å, *c* = 20.3030(16) Å, *α* = 98.8240(10)°, *β* = 104.7000(10)°, *γ* = 101.0710(10)°, *V* = 2262.8(3) Å^3, *Z* = 2, D_{calcd} = 1.789 Mg m^{-3}, *μ* = 1.901 mm^{-1}, *T* = 293(2) K, crystal size 0.42 × 0.21 × 0.10 mm; reflections collected 12538, independent reflections 8843; 5779 with $I > 2\sigma(I)$; *R*1 = 0.0641 [$I > 2\sigma(I)$], w*R*2 = 0.1638 [$I > 2\sigma(I)$]; *R*1 = 0.1063 (all data), w*R*2 = 0.1860 (all data), GOF (on F^2) = 1.038.

Spectral Characterization of 2c. Positive ESI FT-ICR MS: *m*/*z* calcd for $[M + H]^+$ ($C_{84}H_{13}Br_2^+$) 1178.93785, found 1178.94001. ^{1}H NMR (600 MHz, in CS_2 with benzene-d_6 as the external lock solvent) *δ* = 7.87 (s, 1H), 7.72−7.69 (t, 2H), 7.62−7.59 (t, 2H), 7.55 (s, 1H), 7.45 (t, 1H), 7.36 (d, 1H), 3.64 (AB_q , Δ*ν* = 30.0 Hz, J_{AB} = 12.0 Hz, 2H), 3.21(AB_q, Δ*ν* = 24.0 Hz, J_{AB} = 12.0 Hz, 2H). ^{13}C NMR (150 MHz, CS_2/$CDCl_3$) all signals represent 1C except noted: *δ*=168.71, 159.70, 156.53, 154.76, 151.76, 151.58, 150.85, 150.39, 150.18, 149.68 (2C), 149.62, 149.07 (2C), 148.91, 148.77, 148.45, 148.35, 148.00, 147.76, 147.70, 147.61 (2C), 147.52, 147.40, 147.36, 146.97, 146.64, 146.51 (2C), 146.27, 146.09, 145.98, 145.63, 145.58, 145.40, 145.19, 145.11, 144.90, 144.77, 144.46, 144.42, 144.18, 143.85, 143.75, 143.58, 143.55, 142.90 (2C), 142.84, 142.66, 142.56, 142.39, 142.23, 141.51, 138.89, 138.77, 138.58, 137.13, 136.98, 135.88, 134.19, 133.67 (Ph), 133.38 (Ph), 132.83, 132.79, 132.61, 132.23, 131.14, 130.80, 130.56 (Ph), 130.50 (Ph), 129.87 (Ph), 129.62 (Ph), 129.47 (Ph), 129.12 (Ph), 128.80 (Ph), 127.88 (Ph), 122.78 (Ph), 122.50 (Ph), 57.36 (sp^3, C_{70}), 55.76 (sp^3, C_{70}), 46.27 (CH_2), 42.81 (CH_2). UV−vis (toluene): λ_{max}/nm = 355, 415, 602, and 701.

Spectral Characterization of 1d. Positive ESI FT-ICR MS: *m*/*z* calcd for $[M + H]^+$ ($C_{84}H_{13}Br_2^+$) 1178.93785, found 1178.93607. ^{1}H NMR (600 MHz, in CS_2 with benzene-d_6 as the external lock solvent) *δ*= 7.32 (d, 4H), 7.06 (d, 4H), 3.48 (AB_q, Δ*ν* = 18.0 Hz, *J* = 12.0 Hz, 4H). ^{13}C NMR (125 MHz, CS_2/$CDCl_3$): *δ* = 157.72 (2C), 150.96 (2C), 150.75 (2C), 150.52 (2C), 149.94 (2C), 148.91 (2C), 148.87 (2C), 148.84 (2C), 148.48 (2C), 148.47 (2C), 147.47 (2C), 147.35 (2C), 147.18 (4C), 147.01 (2C), 146.22 (2C), 146.06 (2C), 145.42 (2C), 145.37 (4C), 144.79 (2C), 144.64 (2C), 144.51 (2C), 143.90 (2C), 143.06 (2C), 142.71 (2C), 142.36 (2C), 141.23 (2C), 139.87 (2C), 139.20 (2C), 134.56 (2C, Ph), 134.22 (2C), 134.19 (2C), 133.71 (2C), 132.15 (4C, Ph), 132.12 (2C), 131.67 (4C, Ph), 122.55 (2C, Ph), 57.05 (2C, sp^3, C_{70}), 49.46 (2C, CH_2). UV−vis (toluene): λ_{max}/nm = 403, 438, 624, and 785.

Spectral Characterization of 2d. Positive ESI FT-ICR MS: *m*/*z* calcd for $[M + H]^+$ ($C_{84}H_{13}Br_2^+$) 1178.93785, found 1178.93639. ^{1}H NMR (600 MHz, in CS_2 with C_6D_6 as the external lock solvent) *δ* = 7.82 (d, 2H), 7.64 (d, 4H), 7.28 (d, 2H), 3.72 (AB_q, Δ*ν* = 30.0 Hz, J_{AB} = 12.0 Hz, 2H), 3.28 (AB_q, Δ*ν* = 18.0 Hz, J_{AB} = 12.0 Hz, 2H). ^{13}C NMR (150 MHz, CS_2/$CDCl_3$) all signals represent 1C except noted: *δ* = 168.48, 159.67, 156.64, 154.91, 151.76, 151.58, 150.95, 150.37, 150.14, 149.67 (2C), 149.61, 149.07 (2C), 148.88, 148.77, 148.43, 148.35, 148.01, 147.75, 147.69, 147.62, 147.60, 147.51, 147.40, 147.35, 146.95, 146.79, 146.52, 146.50, 146.27, 146.08, 145.96, 145.58 (2C), 145.40, 145.18, 145.04, 144.87, 144.76, 144.44, 144.40, 144.16, 143.79, 143.72, 143.58, 143.55, 142.89, 142.84, 142.71, 142.65, 142.39, 142.20, 141.51, 138.74, 137.12, 137.03, 135.91, 135.51 (Ph), 135.11 (Ph), 134.19, 132.83, 132.77, 132.59, 132.30 (2C, Ph), 132.22, 132.06 (2C), 131.96 (2C, Ph), 131.56 (2C, Ph), 131.42 (2C), 131.28 (2C, Ph), 131.13, 121.84 (Ph), 121.72 (Ph), 57.37 (sp^3, C_{70}), 55.76 (sp^3, C_{70}), 46.39 (CH_2), 42.96 (CH_2). UV−vis (toluene): λ_{max} = 355, 415, 602, and 701.

X-ray Single-Crystal Diffraction of 2d. Black crystals of **2d** were obtained by slowly diffusing *n*-hexane into a CS_2 solution of **1c** at room temperature. Single-crystal X-ray diffraction data were collected on an instrument equipped with a CCD area detector using graphite-monochromated Mo K*α* radiation (*λ* = 0.71073 Å) in the scan range $0.81° < \theta < 25.03°$. The structure was solved with the direct method of SHELXS-97 and refined with full-matrix least-squares techniques using the SHELXL-97 program within WINGX. Crystal data of **2d**·2CS_2: $C_{84}H_{12}Br_2$·2CS_2, M_w = 1333.02, Orthorhombic, space group *Pbcn*, *a* = 50.558(3) Å, *b* = 10.0753(6) Å, *c* = 20.1387(12) Å, *α* = 90°, *β* = 90°, *γ* = 90°, *V* = 10258.4(10) Å^3, *Z* = 8, D_{calcd} = 1.726 Mg m^{-3}, *μ* = 1.803 mm^{-1}, *T* = 293(2) K, crystal size 0.38 × 0.26 × 0.14 mm; reflections collected 49745, independent reflections 9025; 5935 with $I > 2\sigma(I)$; *R*1 = 0.0717 [$I > 2\sigma(I)$], w*R*2 = 0.1797 [$I > 2\sigma(I)$]; *R*1 = 0.1158(all data), w*R*2 = 0.2041 (all data), GOF (on F^2) = 1.053.

H/D Labeling Experiment. Route 1: Typically, 150 mg (0.18 mmol) of C_{70} was electrolyzed at −1.10 V vs SCE in 100 mL of freshly distilled PhCN solution containing 0.1 M TBAP under an argon atmosphere. The potentiostat was switched off after the electrolytic formation of C_{70}^{2-} was achieved. Then a 10-fold excess of $PhCD_2Br$ (1.8 mmol, 213 *μ*L) and a 10-fold excess of $PhCH_2Br$ (1.8 mmol, 213 *μ*L) were added simultaneously into the reaction mixture to react for 3 h with stirring at 50 °C. The workup for the purification of **2e** is the same as that for **2a**. Route 2: Typically, 150 mg (0.18 mmol) of C_{70} was electrolyzed at −1.10 V vs SCE in 100 mL of freshly distilled PhCN solution containing 0.1 M TBAP under an argon atmosphere. The potentiostat was switched off after the electrolytic formation of C_{70}^{2-} was complete. A 10-fold excess of $PhCD_2Br$ (1.8 mmol, 213 *μ*L) was added into the solution, and the reaction was allowed to proceed for 20 min, followed by adding a 10-fold excess of $PhCH_2Br$ (1.8 mmol, 213 *μ*L). The reaction was allowed to proceed for about 3 h with stirring at 50 °C. The workup for the purification of **2f** is the same as that for **2a**.

Spectral Characterization of 2e. ^{1}H NMR (600 MHz, in CS_2 with benzene-d_6 as the external lock solvent): *δ* = 7.75 (d, 2H), 7.71 (t, 2H), 7.58 (t, 1H), 7.58 (t, 2H), 7.47 (t, 1H), 7.40 (d, 2H), 3.68 (s, 1.00H), 3.23 (AB_q, Δ*ν* = 24.0 Hz, *J* = 18.0 Hz, 1.02H).

Spectral Characterization of 2f. ^{1}H NMR (600 MHz, in CS_2 with benzene-d_6 as the external lock solvent): *δ* = 7.72 (d, 2H), 7.68 (t, 2H), 7.56 (t, 1H), 7.52 (t, 2H), 7.44 (t, 1H), 7.38 (d, 2H), 3.66 (s, 0.28H), 3.21 (AB_q, Δ*ν* = 24.0 Hz, *J* = 12.0 Hz, 1.32H).

Computational Methods. The geometry of 2,5-$(PhCH_2)_2C_{70}$ was optimized with Gaussian03 at the Hartree−Fock (HF) level with the 6-31G basis set, followed by harmonic frequency calculations at the same level to confirm them as the energy minima. DFT calculations with Guassian03 were performed at the B3LYP/6-311G(d) level to evaluate the barriers for rotating the benzyls of simulated structures of 2,5-$(PhCH_2)HC_{70}$ and 2,5-$H(PhCH_2)C_{70}$, and the barriers for rotating the phenyl rings of 2,5-$(PhCH_2)_2C_{70}$.

■ ASSOCIATED CONTENT

Ⓢ Supporting Information

X-ray crystallographic files for compounds **1b**,**c** and **2a**,**d** (CIF), HPLC of the crude product, HRMS, UV−vis, ^{1}H and ^{13}C NMR spectra of compounds **1a**−**d** and **2a**−**d**, HMBC NMR spectrum of compounds **2a** and **2b**, ^{1}H NMR of deuterated compounds **2e** and **2f**, and calculation details. This material is available free of charge via the Internet at http://pubs.acs.org.

■ AUTHOR INFORMATION

Corresponding Author

*E-mail: xgao@ciac.jl.cn.

Notes

The authors declare no competing financial interest.

■ ACKNOWLEDGMENTS

This work was supported by NSFC (20972150, 21172212 for X.G. and 21202157 for Z.J.L.) and the Solar Energy Initiative of the CAS (KGCX2-YW-399 + 9).

■ REFERENCES

(1) Caron, C.; Subramanian, R.; D'Souza, F.; Kim, J.; Kunter, W.; Jones, M. T.; Kadish, K. M. *J. Am. Chem. Soc.* **1993**, *115*, 8505−8506.
(2) Boulas, P. L.; Zuo, Y.; Echegoyen, L. *Chem. Commun.* **1996**, 1547−1548.

(3) Kadish, K. M.; Gao, X.; Van Caemelbecke, E.; Hirasaka, T.; Suenobu, T.; Fukuzumi, S. *J. Phys. Chem. A* **1998**, *102*, 3898−3906.
(4) Zheng, M.; Li, F.-F.; Shi, Z.; Gao, X.; Kadish, K. M. *J. Org. Chem.* **2007**, *72*, 2538−2542.
(5) Yang, W.-W.; Li, Z.-J.; Gao, X. *J. Org. Chem.* **2010**, *75*, 4086−4094.
(6) Yang, W.-W.; Li, Z.-J.; Li, F.-F.; Gao, X. *J. Org. Chem.* **2011**, *76*, 1384−1389.
(7) Chen, J.; Cai, R.-F.; Huang, Z.-E.; Wu, H.-M.; Jiang, S.-K.; Shao, Q.-F. *J. Chem. Soc., Chem. Commun.* **1995**, 1553−1554.
(8) Subramanian, R.; Kadish, K. M.; Vijayashree, M. N.; Gao, X.; Jones, M. T.; Miller, M. D.; Krause, K. L.; Suenobu, T.; Fukuzumi, S. *J. Phys. Chem.* **1996**, *100*, 16327−16335.
(9) Bergosh, R. G.; Meier, M. S.; Cooke, J. A. L.; Spielmann, H. P.; Weedon, B. R. *J. Org. Chem.* **1997**, *62*, 7667−7672.
(10) Fukuzumi, S.; Suenobu, T.; Hirasaka, T.; Arakawa, R.; Kadish, K. M. *J. Am. Chem. Soc.* **1998**, *120*, 9220−9227.
(11) Allard, E.; Rivière, L.; Delaunay, J.; Dubois, D.; Cousseau, J. *Tetrahedron. Lett.* **1999**, *40*, 7223−7226.
(12) Allard, E.; Delaunay, J.; Cheng, F.; Cousseau, J.; Ordúna, J.; Garín, J. *Org. Lett.* **2001**, *3*, 3503−3506.
(13) Cheng, F.; Murata, Y.; Komatsu, K. *Org. Lett.* **2002**, *4*, 2541−2544.
(14) Allard, E.; Delaunay, J.; Cousseau, J. *Org. Lett.* **2003**, *5*, 2239−2242.
(15) Allard, E.; Cheng, F.; Chopin, S.; Delaunay, J.; Rondeaub, D.; Cousseau, J. *New J. Chem.* **2003**, *27*, 188−192.
(16) Kadish, K. M.; Gao, X.; Gorelik, O.; Van Caemelbecke, E.; Suenobu, T.; Fukuzumi, S. *J. Phys. Chem. A* **2000**, *104*, 2902−2907.
(17) Ni, L.; Chang, W.-W.; Hou, H.-L.; Li, Z.-J.; Gao, X. *Org. Biomol. Chem.* **2011**, *9*, 6646−6653.
(18) Ni, L.; Yang, W.-W.; Li, Z.-J.; Wu, D.; Gao, X. *J. Org. Chem.* **2012**, *77*, 7299−7306.
(19) Spielmann, H. P.; Wang, G.-W.; Meier, M. S.; Weedon, B. R. *J. Org. Chem.* **1998**, *63*, 9865−9871.
(20) Spielmann, H. P.; Weedon, B. R.; Meier, M. S. *J. Org. Chem.* **2000**, *65*, 2755−2758.
(21) Meier, M. S.; Bergosh, R. G.; Gallagher, M. E.; Spielmann, H. P.; Wang, Z. *J. Org. Chem.* **2002**, *67*, 5946−5952.
(22) Wang, Z.; Meier, M. S. *J. Org. Chem.* **2003**, *68*, 3043−3048.
(23) Li, F.-F.; Rodríguez-Fortea, A.; Poblet, J. M.; Echegoyen, L. *J. Am. Chem. Soc.* **2011**, *133*, 2760−2765.
(24) Li, F.-F.; Rodríguez-Fortea, A.; Peng, P.; Chavez, G. A. C.; Poblet, J. M.; Echegoyen, L. *J. Am. Chem. Soc.* **2012**, *134*, 7480−7487.
(25) Hirsch, A.; Brettreich, M. *Fullerenes: Chemistry and Reactions*; Wiley-VCH Verlag: Weinheim, 2005.
(26) Echegoyen, L.; Echegoyen, L. E. *Acc. Chem. Res.* **1998**, *31*, 593−601.
(27) Diederich, F.; Thilgen, C. *Science* **1996**, *271*, 317−323.
(28) Thilgen, C.; Diederich, F. *Top. Curr. Chem.* **1999**, *199*, 135−171.
(29) For the numbering of C_{70}, refer to: Godly, E. W.; Taylor, R. *Pure Appl. Chem.* **1997**, *69*, 1411−1434.
(30) The three isomers that were proposed in ref 16 were numbered as the 22,41-, 22,25-, and 22,45-isomers according to the numbering of C_{70} in the paper.
(31) Shu, C.; Slebodnick, C.; Xu, L.; Champion, H.; Fuhrer, T.; Cai, T.; Reid, J. E.; Fu, W.; Harich, K.; Dorn, H. C.; Gibson, H. W. *J. Am. Chem. Soc.* **2008**, *130*, 17755−17760.
(32) Xiao, Z.; Wang, F. D.; Huang, S. H.; Gan, L. B.; Zhou, J.; Yuan, G.; Lu, M. J.; Pan, J. Q. *J. Org. Chem.* **2005**, *70*, 2060−2066.
(33) Dorozhkin, E. I.; Ignat'eva, D. V.; Tamm, N. B.; Goryunkov, A. A.; Khavrel, P. A.; Ioffe, I. N.; Popov, A. A.; Kuvychko, I. V.; Streletskiy, A. V.; Markov, V. Y.; Spandl, J.; Strauss, S. H.; Boltalina, O. V. *Chem.—Eur. J.* **2006**, *12*, 3876−3889.
(34) Smith, A. B., III; Strongin, R. M.; Brard, L.; Furst, G. T.; Romanow, W. J.; Owens, K. G.; Goldschmidt, R. J.; King, R. C. *J. Am. Chem. Soc.* **1995**, *117*, 5492−5502.
(35) Chang, W.-W.; Li, Z.-J.; Gao, X. *Org. Lett.* **2013**, *15*, 1642−1645.
(36) Fukuzumi, S.; Suenobu, T.; Gao, X.; Kadish, K. M. *J. Phys. Chem. A* **2000**, *104*, 2908−2913.
(37) Whitesides, G. M.; Holtz, D.; Roberts, J. D. *J. Am. Chem. Soc.* **1964**, *86*, 2628−2634.
(38) It is noteworthy that in ref 36, it is the free rotation of the benzyls rather than the phenyl rings was attributed to account for the coalesce of the diastereotopic methylene protons of 1,4-$(PhCH_2)_2C_{60}$ at high temperature, and this is the ground for the assignment of the 7,38-adduct, in which the two benzyls are less interacted and are supposed to have a relatively free rotation.
(39) Wang, Z. W.; Meier, M. S. *J. Org. Chem.* **2004**, *69*, 2178−2180.
(40) Martín, N. *Chem. Commun.* **2006**, 2093−2104.